

## Influence of using different types of microreactors on the formation of nanocrystalline BiFeO<sub>3</sub>

Olga V. Proskurina<sup>1,2,a</sup>, Rufat Sh. Abiev<sup>1,2,b</sup>, Vladimir N. Nevedomskiy<sup>1,c</sup>

<sup>1</sup>Ioffe Institute, St. Petersburg, Russia

<sup>2</sup>St. Petersburg State Institute of Technology, St. Petersburg, Russia

<sup>a</sup>proskurinaov@mail.ru, <sup>b</sup>abiev.rufat@gmail.com, <sup>c</sup>nevedom@mail.ioffe.ru

Corresponding author: Olga V. Proskurina, proskurinaov@mail.ru

**ABSTRACT** The influence of the coprecipitation of bismuth and iron hydroxides in microreactors of various types on the formation of nanocrystalline bismuth orthoferrite during the heat treatment of the deposit was described. Free impinging-jets microreactor, microreactor with submerged jets, microreactor with intensively swirling flows were used. It was revealed that nanocrystalline bismuth orthoferrite with the smallest weighted average crystallite size of 12 nm is formed when a microreactor with tangentially swirling flows of reagent solutions is used for coprecipitation of hydroxides. The minimum size of BiFeO<sub>3</sub> crystallites according to transmission electron microscopy data is determined as 3–4 nm.

**KEYWORDS** free impinging-jets microreactor, microreactor with submerged jets, microreactor with intensively swirling flows, nanocrystals, bismuth ferrite.

**ACKNOWLEDGEMENTS** X-ray diffraction studies were performed employing the equipment of the Engineering Center of the St. Petersburg State Institute of Technology. TEM characterization was performed using equipment owned by the Federal Joint Research Center “Material science and characterization in advanced technology”. The authors are grateful to V. V. Gusarov for his attention to the work. The research was supported by the Russian Science Foundation Grant 20-63-47016.

**FOR CITATION** Proskurina O.V., Abiev R.Sh., Nevedomskiy V.N. Influence of using different types of microreactors on the formation of nanocrystalline BiFeO<sub>3</sub>. *Nanosystems: Phys. Chem. Math.*, 2023, **14** (1), 120–126.

### 1. Introduction

The morphology, size and structure of nanoparticles, the presence and amount of impurity phases in a nanopowder can significantly affect the mechanical and functional properties of the materials obtained from them [1–3], including the magnetic, electrical, photocatalytic properties of bismuth orthoferrite [4–11]. These reasons stimulate the development of methods for synthesis of bismuth orthoferrite nanopowders, which would provide their morphological characteristics, dispersed and phase composition, necessary to obtain materials with needed properties.

There are several methods for synthesis of bismuth orthoferrite nanoparticles, for example, solution combustion [12–20], hydrothermal synthesis [21–27], and solid phase synthesis [28–35]. However, obtaining single-phase nanocrystalline powders based on bismuth orthoferrite still causes difficulties [28, 36–40]. One of the ways to obtain oxide nanoparticles with a given composition and size is the use of microreactors [41, 42].

For example, the synthesis of nanocrystals of complex oxides using free impinging-jets microreactors demonstrated promising results [43–47]. Free impinging-jets microreactors make it possible to dissipate a large amount of energy in very small volumes [48]. This, under certain flow regimes of free impinging-jets of reagent solutions, leads to the formation of reaction zones with sizes of the order of hundreds of nanometers with localization of the initial components in them in a given stoichiometry [49]. Such self-organization of spatially separated nanoreactors makes it possible to count on the possibility of forming nanoparticles of a given composition and size [50].

When a free impinging-jets microreactor is used to obtain precursors for the following synthesis of bismuth orthoferrite, as shown in [51–53], the formation of by-products that differ in composition from the stoichiometry of the target phase is almost completely excluded. Comparison of various apparatuses for coprecipitation of precursors were considered in [51], in particular, a microreactor with submerged jets. By use of different types of microreactors, the authors of [51] obtained predominantly single-crystal BiFeO<sub>3</sub> nanoparticles with a narrow size distribution and small average sizes of crystallites and particles. At the same time, these sizes are not always close to the minimum possible sizes of bismuth orthoferrite crystals [54].

Thus, it is important to determine the types of microreactors and synthesis modes for obtaining single-phase nanopowders based on bismuth orthoferrite with the smallest possible crystal sizes. This work is aimed at solving this problem.

## 2. Experimental

The crystalline hydrates of bismuth and iron (III) nitrates were used as starting reagents. Bismuth nitrate  $\text{Bi}(\text{NO}_3)_3 \cdot 5\text{H}_2\text{O}$  was dissolved in 70 mL of 4M  $\text{HNO}_3$  with stirring for 10 minutes and heating to 70 °C. An equimolar amount of iron nitrate  $\text{Fe}(\text{NO}_3)_3 \cdot 9\text{H}_2\text{O}$  was added with stirring to the obtained solution of bismuth nitrate. Salt weights were calculated for the preparation of 3 g of bismuth ferrite. After stirring for 10 minutes, 130 mL of distilled water was added and stirred for another 20 minutes. Separately, 1 l of 4M NaOH solution was prepared. The obtained solutions were used for the coprecipitation of bismuth and iron(III) hydroxides in various types of microreactors. Coprecipitation was carried out at a temperature of about 22 °C and atmospheric pressure.

The design of the microreactor with submerged jets used for intensive mixing of the solutions of the reagents (Fig. 1a) is described in [51]. The reactor was filled with NaOH solution to a level that was kept constant by means of a hydraulic lock. After that, the solutions of nitrates and alkali were fed by means of Heidolph Pumpdrive 5201 peristaltic pumps simultaneously through two nozzles located on opposite walls of the reactor at an angle of 180 degrees to each other. A solution of bismuth and iron nitrates was supplied through one nozzle, 0.52 mm in diameter, and a solution of NaOH was supplied through another nozzle, 0.47 mm in diameter. The flow rate of both solutions was 150 mL/min. The superficial velocity of the jets at the outlet of the nozzles was 15.3 m/s for the salt mixture solution and 16.7 m/s for the alkali solution. When the pumps were started, the nitrate solution was “injected” into the reactor filled with NaOH, and metal hydroxides immediately precipitated. In essence, this method is a variant of intensive reverse precipitation. The particles of co-precipitated hydroxides formed during the chemical reaction were removed through the hydraulic lock hosepipe into a receiving tank.

A free impinging-jets microreactor (Fig. 1b) described in [52, 53] was also used to mix the reagents. A solution of bismuth and iron nitrates was fed into the jet microreactor through one of the nozzles with a diameter of 0.44 mm, and a solution of sodium hydroxide was supplied through the second nozzle with a diameter of 0.46 mm. The solutions were delivered as thin jets at a fixed flow rate of 250 mL/min, colliding at a mean velocity of about 23 m/s in a vertical plane at an angle of about 72 °. The mutual arrangement of the nozzles and the flow rate were set in such a way that the collision of the jets resulted in the formation of a liquid sheet with an average thickness of 10–15  $\mu\text{m}$  [55], in which there was contact and mixing of solutions of the initial components (Fig. 1b). The coprecipitation of bismuth and iron hydroxides in a jet microreactor was carried out for 5–10 ms.

A microreactor with intensively swirling flows (Fig. 1c) makes it possible to concentrate a large amount of kinetic energy in a relatively small volume (about 0.35 mL), which leads to the creation of a high level of specific energy dissipation rate (about 2–35 kW/kg), which, in turn, causes high local values of longitudinal and shear deformation of fluid elements and contributes to the intensification of the micromixing process [56, 57]. The flow rates of each solution at the preliminary stage of the experiment were set at 0.5, 1.0, 2.0, and 3.0 L/min. In this case, nitrate solutions were fed into one of the tangential nozzles, and the precipitant solution was fed into the axial nozzle (Fig. 1c). Since no significant effect of solution flow rates in the range of 0.5–3.0 L/min on the size of crystallites was found (the sizes varied from  $14 \pm 5$  nm for 0.5 L/min to  $12 \pm 5$  nm for 3.0 L/min), then further all studies were carried out for a sample obtained at a flow rate of 3.0 L/min. This result is important from the point of view of crystallite size stability, since it guarantees the production of particles with an average crystallite size in a narrow range, from 12 to 14 nm, with a relatively wide change in solution flow rates, from 0.5 L/min to 3.0 L/min.

As a result of mixing solutions in microreactors, a suspension of co-precipitated bismuth and iron hydroxides was obtained, which was then washed with distilled water from alkali using centrifugation and intermediate dispersion using an ultrasonic bath in order to better wash the precipitates from alkali residues. The washed samples were dried at 70 °C for a day.

The samples were designated as follows: *N1* – obtained using a microreactor with submerged jets, *N2* – using a free impinging-jets microreactor, *N3* – using a microreactor with intensively swirling flows. The samples were heated in a tubular furnace in a platinum crucible at a temperature of 490 °C in the “annealing-hardening” mode for 1 minute.

Powders were characterized by several methods. X-ray diffraction patterns were taken on a Rigaku SmartLab 3 (Rigaku Corporation, Japan) powder diffractometer ( $\text{CuK}\alpha$  radiation) in the angle range  $2\theta = 20\text{--}60^\circ$  with a step of  $0.01^\circ$  and a speed of  $0.1^\circ/\text{min}$ . The phase analysis of the samples was determined using the ICSD PDF-2 database. The average crystallite size was determined using the SmartLab Studio II software package from Rigaku. The size distribution of crystallites was determined by the method of fundamental parameters in the approximation of a lognormal distribution model using the SmartLab Studio II software package for reflection 012.

The elemental composition of the samples was determined using a Tescan Vega 3 SBH scanning electron microscope (Tescan, Czech Republic) with an energy dispersive X-ray spectroscopy (EDX) Oxford Instruments INCA x-act X-ray microanalysis attachment (Oxford Instruments, Oxford, UK).

Transmission electron microscopy (TEM) studies with the determination of microdiffraction of the samples were performed using a JEOL JEM-2100F microscope (JEOL Ltd., Akishima, Tokyo, Japan) at an accelerating voltage of 200 kV. Samples for research were prepared by preliminary dispersion of the initial powder in ethyl alcohol in an ultrasonic bath for 15 minutes, followed by deposition on a supporting film.

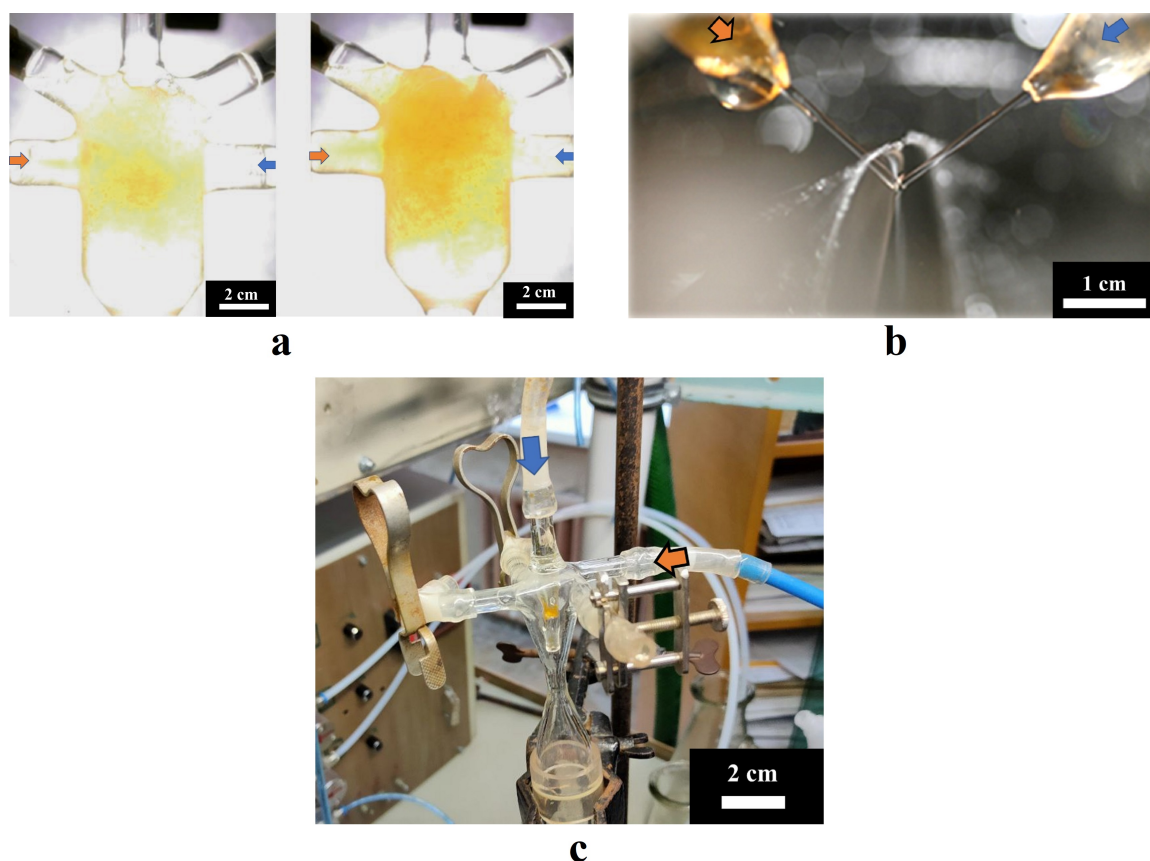


FIG. 1. Microreactors for co-precipitation of bismuth and iron hydroxides: a) with submerged jets; b) free impinging-jets; c) with intensively swirling flows

### 3. Results and discussion

The data of X-ray spectral microanalysis of all samples showed that the ratio of Bi:Fe elements in the samples, within the error limits, corresponds to the ratio specified during synthesis, with respect to the stoichiometry of  $\text{BiFeO}_3$ .

The X-ray diffraction data for the heat-treated samples are shown in Fig. 2. Diffractograms for all three samples before heat treatment, i.e. bismuth and iron hydroxides coprecipitated using different microreactors have the same X-ray

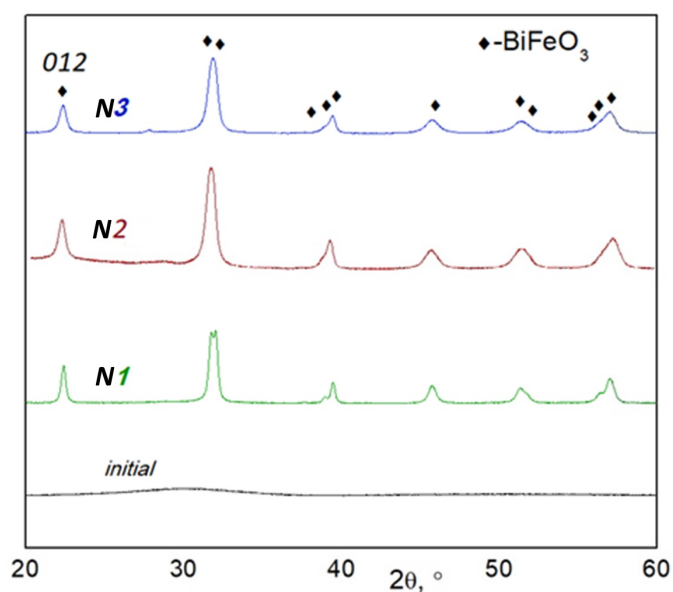


FIG. 2. X-ray diffraction patterns of samples after heat treatment ( $490\text{ }^{\circ}\text{C}$ , 1 min) – N1, N2, N3, and before heat treatment – “initial”

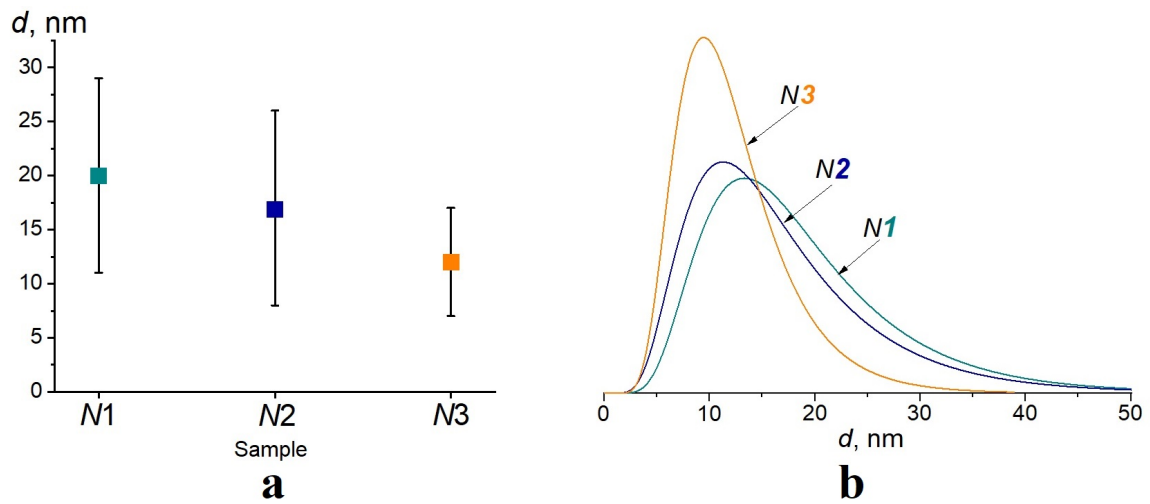


FIG. 3. Average sizes of bismuth orthoferrite crystallites in samples  $N1$ ,  $N2$ ,  $N3$  after heat treatment – a); size distribution of crystallites according to the 012 reflection in samples  $N1$ ,  $N2$ ,  $N3$  – b)

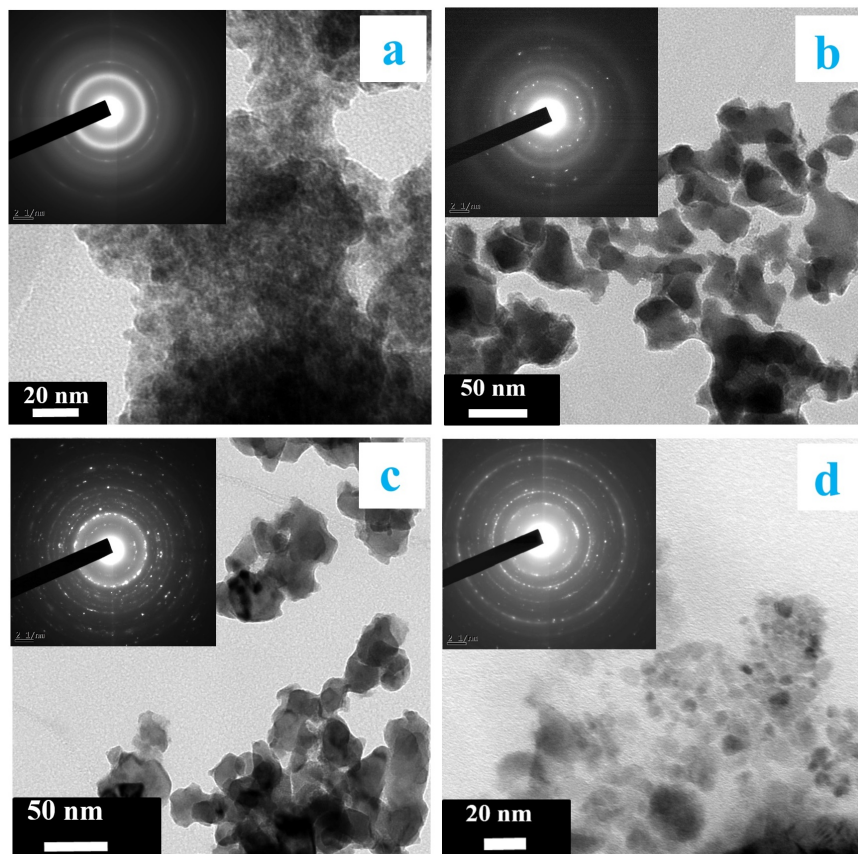


FIG. 4. TEM micrographs: sample “initial” before heat treatment (a); samples after heat treatment:  $N1$  (b),  $N2$  (c),  $N3$  (d)

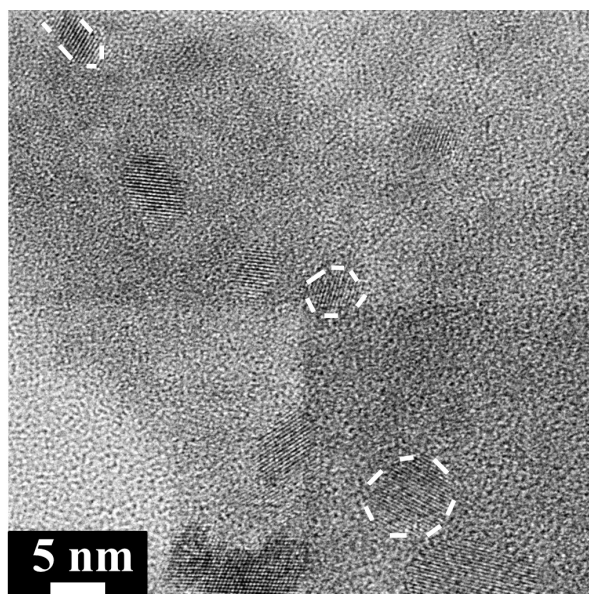


FIG. 5. TEM micrograph of sample *N3*. As an example, three  $\text{BiFeO}_3$  nanocrystals are highlighted in the image

amorphous appearance and are shown in Fig. 2 under the name “initial”. All reflections in the diffraction patterns of samples *N1*, *N2*, and *N3* correspond to the bismuth orthoferrite phase.

Figure 3 shows the average crystallite sizes of the samples (Fig. 3a), as well as the size distributions of crystallites (Fig. 3b), determined from the 012 reflection.

Sample *N3* has the smallest average crystallite size, about 12 nm. The average size of crystallites for sample *N1* is about 19 nm, for sample *N2*, is about 17 nm. The volumetric size distribution of crystallites for sample *N3*, obtained using a microreactor with intensively swirling flows, is narrower ( $\sigma = 5$  nm) than that for samples *N1* and *N2* ( $\sigma = 9$  nm), obtained using microreactors with free impinging-jets and submerged jets.

A micrograph of the *N2* sample before heat treatment, obtained with a transmission electron microscope, is shown in Fig. 4a. This sample is X-ray amorphous particles collected in aggregates. Pictures of samples *N1*, *N2*, *N3* after heat treatment are shown in Figs. 4b, 4c, 4d, respectively. The electron microdiffraction data confirm the polycrystalline nature of the samples, as well as the presence of some X-ray amorphous phase.

Figure 5 shows a micrograph of sample *N3*, which shows the crystallites of bismuth orthoferrite formed in the amorphous phase. The minimum size of  $\text{BiFeO}_3$  crystallites from transmission electron microscopy data can be estimated as approximately 3–4 nm.

The formation of nanocrystalline bismuth orthoferrite can be explained within the framework of the mechanism of self-organization of spatial restrictions on the growth of particles [50] arising in Kolmogorov-scale vortices in various types of microreactors. In this case, Kolmogorov vortices act as nanoreactors, in which, in this case, nanoparticles of bismuth and iron hydroxides are formed, which are precursors for the synthesis of  $\text{BiFeO}_3$  during their dehydration.

For the synthesis of nanoparticles with the smallest possible sizes under the conditions of the formation of such spatial restrictions, it is important to organize a large contact surface of the reagents and quickly remove the products of interaction from the reaction zone, which is facilitated by the use of microreactor technique.

#### 4. Conclusion

The presented data allow us to conclude that the use of various types of microreactors makes it possible to obtain a nanocrystalline single-phase powder based on bismuth orthoferrite. The smallest average size of  $\text{BiFeO}_3$  crystallites (about 12 nm) was observed in the sample obtained using a microreactor with intensively swirling flows with a reagent flow rate of 3.0 L/min. From the point of view of the stability of the obtained nanocrystalline  $\text{BiFeO}_3$  samples, this result is positive, since under production conditions it guarantees the production of nanocrystalline  $\text{BiFeO}_3$  with an average crystallite size of  $12 \pm 5$  nm within a wide range of the solutions flow rates, from 0.5 L/min to 3.0 L/min.

#### References

- [1] Kushwaha A.K., John M., Misra M., Menezes P.L. Nanocrystalline Materials: Synthesis, Characterization, Properties, and Applications. *Crystals*, 2021, **11**(11), P. 1317.
- [2] Wongkaew N., Simsek M., Griesche C., Baeumner A.J. Functional Nanomaterials and Nanostructures Enhancing Electrochemical Biosensors and Lab-on-a-Chip Performances: Recent Progress, Applications, and Future Perspective. *Chemical Reviews*, 2019, **119**(1), P. 120–194.

- [3] Gupta D., Varghese B.S., Suresh M., Panwar C., Gupta T.K. Nanoarchitectonics: functional nanomaterials and nanostructures – a review. *Journal of Nanoparticle Research*, 2022, **24**, P. 196.
- [4] Lomanova N.A., Panchuk V.V., Semenov V.G., Pleshakov I.V., Volkov M.P., Gusarov V.V. Bismuth orthoferrite nanocrystals: magnetic characteristics and size effects. *Ferroelectrics*, 2020, **569**(1), P. 240–250.
- [5] Wang N., Luo X., Han L., Zhang Z., Zhang R., Olin H., Yang Y. Structure, Performance, and Application of BiFeO<sub>3</sub> Nanomaterials. *Nano-Micro Letters*, 2020, **12**, P. 81.
- [6] Aishwarya K., Hannah Jeniffer I., Maruthasalamoorthy S., Nirmala R., Punithavelan N., Navamathavan R. Review State of the Art of the Multifunctional Bismuth Ferrite: Synthesis Method and Applications. *ECS Journal of Solid State Science and Technology*, 2022, **11**(4), P. 043010.
- [7] Kim S., Nam H., Calisir I. Lead-Free BiFeO<sub>3</sub>-Based Piezoelectrics: A Review of Controversial Issues and Current Research State. *Materials*, 2022, **15**(13), P. 4388.
- [8] Gao T., Chen Z., Huang Q., Niu F., Huang X., Qin L., Huang Y. A review: preparation of bismuth ferrite nanoparticles and its applications in visible-light induced photocatalyses. *Reviews on Advanced Materials Science*, 2015, **40**(2), P. 97–109.
- [9] Irfan S., Zhuanghao Z., Li F., Chen Y.-X., Liang G.-X., Luo J.-T., Ping F. Critical review: Bismuth ferrite as an emerging visible light active nanostructured photocatalyst. *Journal of Materials Research and Technology*, 2019, **8**(6), P. 6375–6389.
- [10] Chien S.-W. C., Ng D.-Q., Kumar D., Lam S.-M., Jaffari Z.H. Investigating the effects of various synthesis routes on morphological, optical, photoelectrochemical and photocatalytic properties of single-phase perovskite BiFeO<sub>3</sub>. *Journal of Physics and Chemistry of Solids*, 2022, **160**, P. 110342.
- [11] Egorysheva A.V., Kraev A.S., Gajtko O.M., Baranchikov A.E., Agafonov A.V., Ivanov V.K. Electrorheological Fluids Based on Bismuth Ferrites BiFeO<sub>3</sub> and Bi<sub>2</sub>Fe<sub>4</sub>O<sub>9</sub>. *Russian Journal of Inorganic Chemistry*, 2020, **65**(8), P. 1253–1263.
- [12] Lomanova N.A., Tomkovich M.V., Sokolov V.V., Gusarov V.V. Special Features of Formation of Nanocrystalline BiFeO<sub>3</sub> via the Glycine-Nitrate Combustion Method. *Russian Journal of General Chemistry*, 2016, **86**(10), P. 2256–2262.
- [13] Lomanova N.A., Tomkovich M.V., Sokolov V.V., Ugolokov V.L., Panchuk V.V., Semenov V.G., Pleshakov I.V., Volkov M.P., Gusarov V.V. Thermal and magnetic behavior of BiFeO<sub>3</sub> nanoparticles prepared by glycine-nitrate combustion. *Journal of Nanoparticle Research*, 2018, **20**, P. 17.
- [14] Lomanova N.A., Tomkovich M.V., Danilovich D.P., Osipov A.V., Panchuk V.V., Semenov V.G., Pleshakov I.V., Volkov M.P., Gusarov V.V. Magnetic Characteristics of Nanocrystalline BiFeO<sub>3</sub>-Based Materials Prepared by Solution Combustion Synthesis. *Inorganic Materials*, 2020, **56**(12), P. 1271–1277.
- [15] Verma R., Chauhan A., Neha, Batoo K.M., Kumar R., Hadhi M., Raslan E.H. Effect of calcination temperature on structural and morphological properties of bismuth ferrite nanoparticles. *Ceramics International*, 2021, **47**(3), P. 3680–3691.
- [16] Mhamad S.A., Ali A.A., Mohtar S.S., Aziz F., Aziz M., Jaafar J., Yusof N., Salleh W.N.W., Ismail A.F., Chandren S. Synthesis of bismuth ferrite by sol-gel auto combustion method: Impact of citric acid concentration on its physicochemical properties. *Materials Chemistry and Physics*, 2022, **282**, P. 125983.
- [17] Asefi N., Masoudpanah S.M., Hasheminasari M. Photocatalytic performances of BiFeO<sub>3</sub> powders synthesized by solution combustion method: The role of mixed fuels. *Materials Chemistry and Physics*, 2019, **228**, P. 168–174.
- [18] Parvathy N.S., Govindaraj R. Atomic scale insights on the growth nanoparticles of BiFeO<sub>3</sub> nanoparticles. *Scientific Reports*, 2022, **12**, P. 4758.
- [19] Alikhanov N.M.-R., Rabadanov M.Kh., Orudzhev F.F., Gadzhimagomedov S.Kh., Emirov R.M., Sadykov S.A., Kallaev S.N., Ramazanov S.M., Abdulvakhidov K.G., Sobola D. Size-dependent structural parameters, optical, and magnetic properties of facile synthesized pure-phase BiFeO<sub>3</sub>. *Journal of Materials Science: Materials in Electronics*, 2021, **32**, P. 13323–13335.
- [20] Ortiz-Quirionez J.-L., Pal U., Villanueva M.S. Effects of Oxidizing/Reducing Agent Ratio on Phase Purity, Crystallinity, and Magnetic Behavior of Solution-Combustion-Grown BiFeO<sub>3</sub> Submicroparticles. *Inorganic Chemistry*, 2018, **57**(10), P. 6152–6160.
- [21] Proskurina O.V., Tomkovich M.V., Bachina A.K., Sokolov V.V., Danilovich D.P., Panchuk V.V., Semenov V.G., Gusarov V.V. Formation of Nanocrystalline BiFeO<sub>3</sub> under Hydrothermal Conditions. *Russian Journal of General Chemistry*, 2017, **87**(11), P. 2507–2515.
- [22] Rouhani Z., Karimi-Sabet J., Mehdipourghazi M., Hadi A., Dastbaz A. Response surface optimization of hydrothermal synthesis of Bismuth ferrite nanoparticles under supercritical water conditions: Application for photocatalytic degradation of Tetracycline. *Environmental Nanotechnology, Monitoring & Management*, 2019, **11**, P. 100198.
- [23] Wang Z.-B., Aldalbah A., Ahamad T., Alshehri S.M., Feng P.X. Preparation of BiFeO<sub>3</sub> and its photoelectric performance as photoanode of DSSC. *Ceramics International*, 2021, **47**(19), P. 27565–27570.
- [24] Duan Q., Kong F., Han X., Jiang Y., Liu T., Chang Y., Zhou L., Qin G., Zhang X. Synthesis and characterization of morphology-controllable BiFeO<sub>3</sub> particles with efficient photocatalytic activity. *Materials Research Bulletin*, 2019, **112**, P. 104–108.
- [25] Xu Y., Gao Y., Xing H., Zhang J. Room temperature spontaneous exchange bias in BiFeO<sub>3</sub> micro/nano powders synthesized by hydrothermal method. *Ceramics International*, 2018, **44**(14), P. 17459–17463.
- [26] Huang J., Tan G., Yang W., Zhang L., Ren H., Xia A. Microwave hydrothermal synthesis of BiFeO<sub>3</sub>: Impact of different surfactants on the morphology and photocatalytic properties. *Materials Science in Semiconductor Processing*, 2014, **25**, P. 84–88.
- [27] da Cruz Severo E., Dotto G.L., Silvestri S., dos Santos Nunes I., da Silveira Salla J., Martinez-de la Cruz A., da Boit Martinello K., Foletto E.L. Improved catalytic activity of EDTA-modified BiFeO<sub>3</sub> powders for remarkable degradation of procion red by heterogeneous photo-Fenton process. *Journal of Environmental Chemical Engineering*, 2020, **8**(4), P. 103853.
- [28] Morozov M.I., Lomanova N.A., Gusarov V.V. Specific features of BiFeO<sub>3</sub> formation in a mixture of bismuth(III) and iron(III) oxides. *Russian Journal of General Chemistry*, 2003, **73**, P. 1676–1683.
- [29] Lomanova N.A., Gusarov V.V. Influence of synthesis temperature on BiFeO<sub>3</sub> nanoparticles formation. *Nanosystems: Physics, Chemistry, Mathematics*, 2013, **4**(5), P. 696–705.
- [30] Tuluk A., Brouwer H., van der Zwaag S. Controlling the Oxygen Defects Concentration in a Pure BiFeO<sub>3</sub> Bulk Ceramic. *Materials*, 2022, **15**, P. 6509.
- [31] Rojac T., Bencan A., Malic B., Tutuncu G., Jones J.L., Daniels J.E., Damjanovic D. BiFeO<sub>3</sub> Ceramics: Processing, Electrical, and Electromechanical Properties. *Journal of the American Ceramic Society*, 2014, **97**(7), P. 1993–2011.
- [32] Yao Y., Ploss B., Mak C.L., Wong K.H. Pyroelectric properties of BiFeO<sub>3</sub> ceramics prepared by a modified solid-state-reaction method. *Applied Physics A*, 2010, **99**, P. 211–216.
- [33] Han H., Lee J.H., Jang H.M. Low-Temperature Solid-State Synthesis of High-Purity BiFeO<sub>3</sub> Ceramic for Ferroic Thin-Film Deposition. *Inorganic Chemistry*, 2017, **56**(19), P. 11911–11916.
- [34] Carranza-Celis D., Cardona-Rodríguez A., Narváez J., Moscoso-Londono O., Muraca D., Knobel M., Ornelas-Soto N., Reiber A., Ramírez J.G. Control of Multiferroic properties in BiFeO<sub>3</sub> nanoparticles. *Scientific Reports*, 2019, **9**, P. 3182.
- [35] Gil-González E., Perejón A., Sónchez-Jiménez P.E., Sayagués M.J., Raj R., Pérez-Maqueada L.A. Phase-pure BiFeO<sub>3</sub> produced by reaction flash-sintering of Bi<sub>2</sub>O<sub>3</sub> and Fe<sub>2</sub>O<sub>3</sub>. *Journal of Materials Chemistry A*, 2018, **6**(13), P. 5356–5366.

- [36] Selbach S.M., Einarsrud M.-A., Grande T. On the Thermodynamic Stability of BiFeO<sub>3</sub>. *Chemistry of Materials*, 2009, **21**(1), P. 169–173.
- [37] Perdomo C.P.F., Suarez A.V., Gunnewiek R.F.K., Kiminami R.H.G.A. Low temperature synthesis of high purity nanoscaled BiFeO<sub>3</sub> by a fast polymer solution method and their ferromagnetic behavior. *Journal of Alloys and Compounds*, 2020, **849**, P. 156564.
- [38] Silva J., Reyes A., Esparza H., Camacho H., Fuentes L. BiFeO<sub>3</sub>: A Review on Synthesis, Doping and Crystal Structure. *Integrated Ferroelectrics*, 2011, **126**(1), P. 47–59.
- [39] Denisov V.M., Belousova N.V., Zhereb V.P., Denisova L.T., Skorikov V.M. Oxide Compounds of Bi<sub>2</sub>O<sub>3</sub>–Fe<sub>2</sub>O<sub>3</sub> System I. The Obtaining and Phase Equilibriums. *Journal of Siberian Federal University. Chemistry*, 2012, **5**(2), P. 146–167.
- [40] Pikula T., Szumiata T., Siedliska K., Mitsiuk V.I., Panek R., Kowalczyk M., Jartych E. The Influence of Annealing Temperature on the Structure and Magnetic Properties of Nanocrystalline BiFeO<sub>3</sub> Prepared by Sol–Gel Method. *Metallurgical and Materials Transactions A*, 2022, **53**, P. 470–483.
- [41] Stankiewicz A.I., Moulijn J.A. Process intensification: Transforming chemical engineering. *Chemical Engineering Progress*, 2000, **96**(1), P. 22–34.
- [42] Abiev R.Sh., Almyasheva O.V., Popkov V.I., Proskurina O.V. Microreactor synthesis of nanosized particles: The role of micromixing, aggregation, and separation processes in heterogeneous nucleation. *Chemical Engineering Research and Design*, 2022, **178**, P. 73–94.
- [43] Marchisio D.L., Rivautella L., Barresi A.A. Design and Scale-Up of Chemical Reactors for Nanoparticle Precipitation. *AIChE Journal*, 2006, **52**(5), P. 1877–1887.
- [44] Kumar R.D.V., Prasad B.L.V., Kulkarni A.A. Impinging Jet Micromixer for Flow Synthesis of Nanocrystalline MgO: Role of Mixing/Impingement Zone. *Industrial Engineering Chemistry Research*, 2013, **52**(49), P. 17376–17382.
- [45] Abiev R.Sh., Almyasheva O.V., Gusarov V.V., Izotova S.G. Method of producing nanopowder of cobalt ferrite and microreactor to this end. RF Patent 2625981, Bull. N 20, 20.07.2017. <https://patents.google.com/patent/RU2625981C1/en>.
- [46] Abiev R.S., Almyasheva O.V., Izotova S.G., Gusarov V.V. Synthesis of cobalt ferrite nanoparticles by means of confined impinging-jets reactors. *Journal Chemical Technology and Applications*, 2017, **1**(1), P. 7–13.
- [47] Abiev R.S. Impinging-Jets Micromixers and Microreactors: State of the Art and Prospects for Use in the Chemical Technology of Nanomaterials (Review). *Theoretical Foundations of Chemical Engineering*, 2020, **54**(6), P. 1131–1147.
- [48] Johnson B.K., Prud'homme R.K. Chemical Processing and Micromixing in Confined Impinging Jets. *AIChE Journal*, 2003, **49**(9), P. 2264–2282.
- [49] Bałdyga J., Jasińska M., Orciuch W. Barium Sulphate Agglomeration in a Pipe – An Experimental Study and CFD Modeling. *Chemical Engineering & Technology*, 2003, **26**(3), P. 334–340.
- [50] Almyasheva O.V., Popkov V.I., Proskurina O.V., Gusarov V.V. Phase formation under conditions of self-organization of particle growth restrictions in the reaction system. *Nanosystems: Physics, Chemistry, Mathematics*, 2022, **13**(2), P. 164–180.
- [51] Proskurina O.V., Sokolova A.N., Sirotkin A.A., Abiev R.Sh., Gusarov V.V. Role of Hydroxide Precipitation Conditions in the Formation of Nanocrystalline BiFeO<sub>3</sub>. *Russian Journal of Inorganic Chemistry*, 2021, **66**(2), P. 163–169.
- [52] Proskurina O.V., Nogovitsin I.V., Il'ina T.S., Danilovich D.P., Abiev R.Sh., Gusarov V.V. Formation of BiFeO<sub>3</sub> Nanoparticles Using Impinging Jets Microreactor. *Russian Journal of General Chemistry*, 2018, **88**(10), P. 2139–2143.
- [53] Proskurina O.V., Abiev R.S., Danilovich D.P., Panchuk V.V., Semenov V.G., Nevedomskiy V.N., Gusarov V.V. Formation of nanocrystalline BiFeO<sub>3</sub> during heat treatment of hydroxides co-precipitated in an impinging-jets microreactor. *Chemical Engineering and Processing – Process Intensification*, 2019, **143**, P. 107598.
- [54] Almyasheva O.V., Lomanova N.A., Popkov V.I., Proskurina O.V., Tugova E.A., Gusarov V.V. The minimal size of oxide nanocrystals: phenomenological thermodynamic vs crystal-chemical approaches. *Nanosystems: Physics, Chemistry, Mathematics*, 2019, **10**(4), P. 428–437.
- [55] Abiev R.S., Sirotkin A.A. Effect of Hydrodynamic Conditions on Micromixing in Impinging-Jets Microreactors. *Theoretical Foundations of Chemical Engineering*, 2022, **56**(1), P. 9–22.
- [56] Abiev R.Sh., Makusheva I.V. Effect of Macro- and Micromixing on Processes Involved in Solution Synthesis of Oxide Particles in Microreactors with Intensively Swirling Flows. *Theoretical Foundations of Chemical Engineering*, 2022, **56**(2), P. 141–151.
- [57] Abiev R.Sh., Makusheva I.V. Energy Dissipation Rate and Micromixing in a Two-Step Micro-Reactor with Intensively Swirled Flows. *Micromachines*, 2022, **13**(11), P. 1859.

---

Submitted 27 September 2022; revised 10 October 2022; accepted 30 October 2022

#### Information about the authors:

*Olga V. Proskurina* – Ioffe Institute, 194021 St. Petersburg, Russia; St. Petersburg State Institute of Technology, 190013 St. Petersburg, Russia; ORCID 0000-0002-2807-375X; proskurinaov@mail.ru

*Rufat Sh. Abiev* – Ioffe Institute, 194021 St. Petersburg, Russia; St. Petersburg State Institute of Technology, 190013 St. Petersburg, Russia; ORCID 0000-0003-3571-5770; abiev.rufat@gmail.com

*Vladimir N. Nevedomskiy* – Ioffe Institute, 194021 St. Petersburg, Russia; ORCID 0000-0002-7661-9155; nevedom@mail.ioffe.ru

*Conflict of interest:* the authors declare no conflict of interest.